NASA Technical Memorandum 109010

15P

Further Studies Using Matched Filter Theory and Stochastic Simulation for Gust Loads Prediction

Robert C. Scott, Anthony S. Pototzky, and Boyd Perry III

July 1993

National Aeronautics and Space Administration

Langley Research Center
Hampton, Virginia 23681-0001

FURTHER STUDIES USING MATCHED FILTER THEORY AND STOCHASTIC SIMULATION FOR GUST LOADS PREDICTION

Robert C. Scott♠
NASA Langley Research Center
Hampton, VA

Anthony S. Pototzky♣
Lockheed Engineering and Sciences Company
Hampton, VA

Boyd Perry III♦
NASA Langley Research Center
Hampton, VA

Abstract

This paper describes two analysis methods -- one deterministic, the other stochastic -- for computing maximized and time-correlated gust loads for aircraft with nonlinear control systems. The first method is based on matched filter theory; the second is based on stochastic simulation. The paper summarizes the methods, discusses the selection of gust intensity for each method and presents numerical results. A strong similarity between the results from the two methods is seen to exist for both linear and nonlinear configurations.

Introduction

For several years NASA Langley Research Center has conducted research in the area of time correlated gust loads and has published a number of papers on the subject (refs. 1-5). The initial research was restricted to mathematically linear systems (refs. 1-3). Recently, however, the focus of the research has been on defining methods that will compute design gust loads for an airplane with a nonlinear control system (refs. 4 and 5). To date, two such methods have been defined: one is based on matched filter theory; the other is based on stochastic simulation.

The Matched-Filter-Based (MFB) Method was developed first and was reported on in reference 4. The MFB Method employs optimization to solve for its answers and this method comes in two varieties: the first uses a one-dimensional search procedure; the second a multi-dimensional search procedure. Based on preliminary results, the first is significantly faster to run and gives design loads only slightly lower in magnitude than the second.

The Stochastic-Simulation-Based (SSB) Method has evolved over the past two years. The SSB Method was presented at a work-in-progress session at an earlier conference (ref. 5) and since then an improvement in the method has been made. The improvement involves what is referred to in the SSB Method as the extraction and averaging procedure. This procedure has been made to be independent of answers from the MFB Method.

The purpose of this paper is to present numerical results recently obtained by applying these two methods. The mathematical model is a model of a current transport aircraft equipped with a nonlinear yaw damper. The model has the same level of complexity as those commonly used in the aircraft industry.

Description of Methods

This section of the paper presents brief descriptions of two analysis methods for computing maximized and time-correlated gust loads for linear and nonlinear airplanes. The first method is the Matched-Filter-Based Method; the second, the Stochastic-Simulation-Based Method.

Matched Filter Based Method

The Matched-Filter-Based (MFB) Method is implemented one way for a linear airplane and two possible ways for a nonlinear airplane.

Implementation for Linear Airplane. A detailed theoretical development of the MFB Method for linear systems can be found in reference 2. The signal flow diagram in figure 1 outlines the implementation and illustrates the intermediate and final products of the process.

Transfer-function representations of atmospheric turbulence and airplane loads are combined in series and represent the "known dynamics" boxes in the figure. A transfer-function representation of the von Karman spectrum in chosen for the gust filter. Load y is the load to be maximized. Loads z_1 through z_n are the loads to be time

♠ Aerospace Engineer, Member AIAA.
♣ Staff Engineer, Senior Member AIAA.
♦ Assistant Head. Aeroservoelasticity Branch.

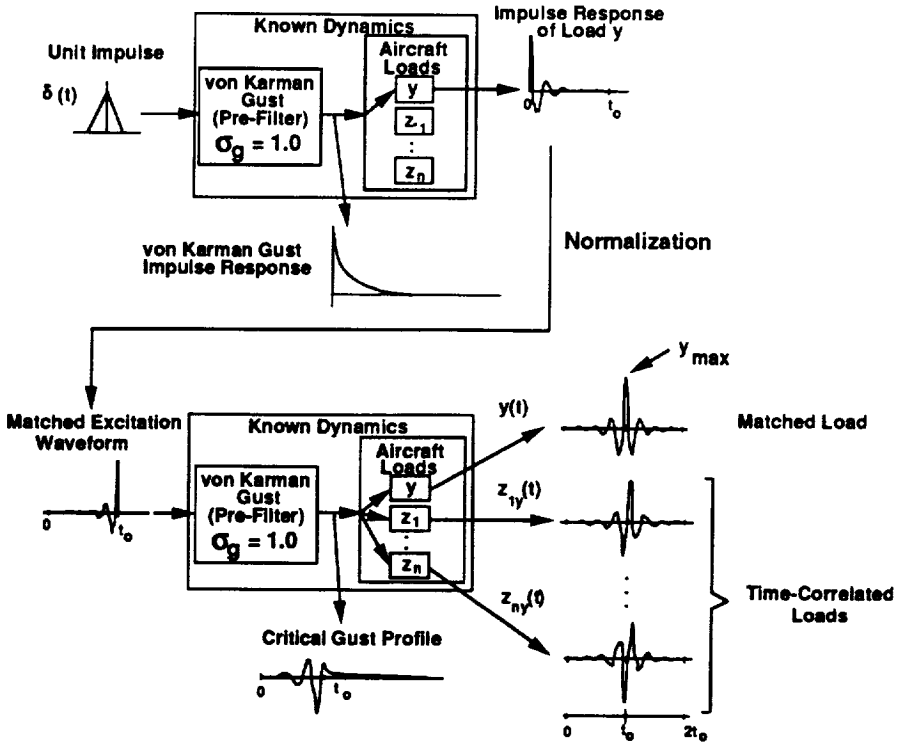

Fig. 1. MFB Linear Method signal flow diagram.

correlated with load y. There are three major steps in the process:

Step 1. The application of an impulse function of unit strength to the combined linear system, producing the impulse response of load y. Based on the time required for the load impulse responses to damp out, a value of t_o is selected. Too large a value will unduly increase the amount of computations required; too small a value will not give accurate answers.

Step 2. The normalization of this impulse response by its own energy, followed by its reversal in time.

Step 3. The application of this normalized reversed signal to the combined linear system, producing time histories of load y and time histories of loads z_1 through z_n. Within the time history of load y, the maximum value is y_{max}. Theory guarantees that there is no other normalized signal that, when applied to the combined linear system, will produce a value of y larger than y_{max}. This guarantee is a fundamental result of the MFB Linear Method

For simplicity of discussion throughout this paper and to avoid confusion between these three steps and the method of reference 6, these three steps will be referred to as the "MFB Linear Method."

Implementation for Nonlinear Airplane - One-Dimensional Search Procedure. A detailed development of the MFB Methods for a nonlinear airplane can be found in reference 4. Figure 2 contains a signal flow diagram of the two possible implementations. Although very similar to figure 1, figure 2 contains some important differences that are indicated by the shaded boxes, quotation marks, and dashed lines.

In figure 2 the initial impulse may have a non-unity strength; the aircraft loads portion of the known dynamics box contains nonlinearities; and the shape of the excitation waveform and the value of y_{max} are functions of the initial impulse strength. In addition, the "matched" excitation waveform and the "matched" load are shown in quotes because, for nonlinear systems, there is no guarantee that y_{max} is a global maximum.

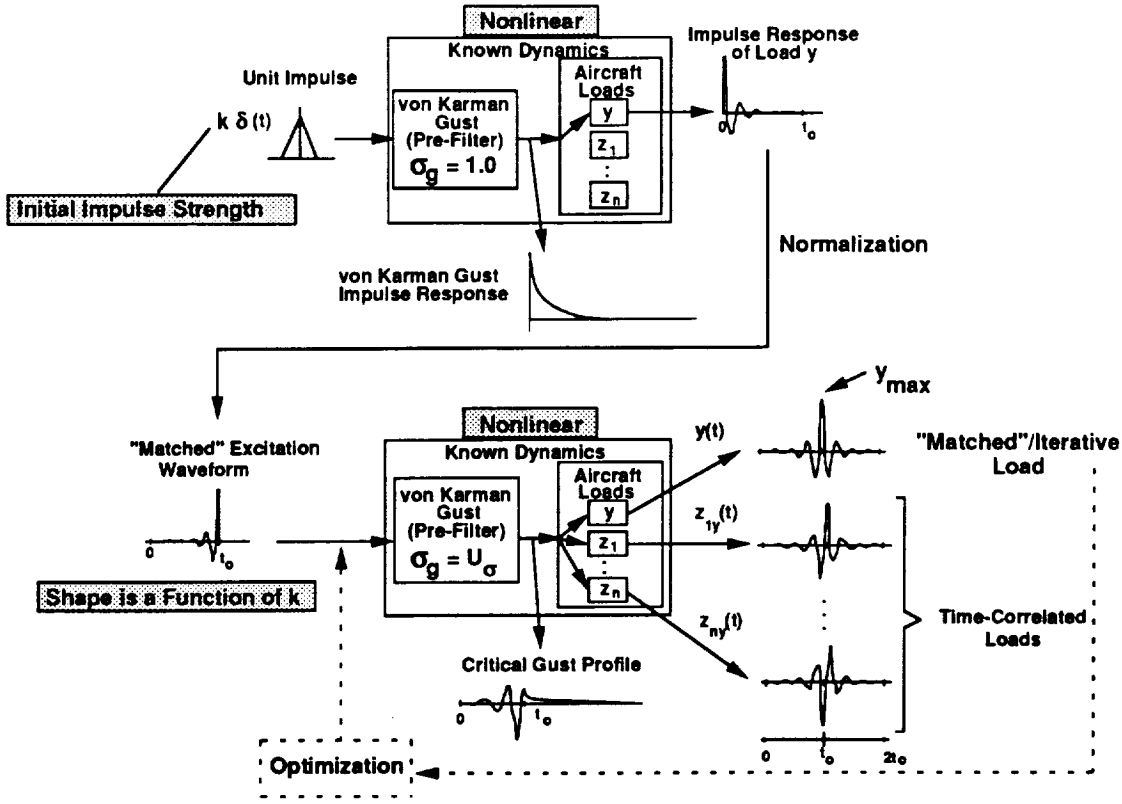

Fig. 2. Nonlinear MFB signal flow diagram for one-dimensional and multi-dimensional searches.

The application of the one-dimensional search procedure is as follows:

Step 1. Select a value of σ_g.

Step 2. Select a range of values of impulse strength, k.

Step 3. Perform steps 1 through 3 of the MFB Linear Method for each value of k, obtaining values of y_{max} and corresponding "matched" excitation waveforms.

Step 4. From these values of y_{max}, select the maximum value of y_{max} and its corresponding "matched" excitation waveform and corresponding impulse strength.

Implementation for Nonlinear Airplane - Multi-Dimensional Search Procedure. The multi-dimensional search procedure uses as its starting point the "matched" excitation waveform from step 4 of the one-dimensional search procedure. In an attempt to obtain an even larger value of y_{max}, a constrained optimization scheme alters the shape but not the energy of the excitation waveform. The waveform is represented by a linear combination of Chebyshev polynomials. The coefficients of the polynomials are the design variables used in the optimization procedure. The converged value of y_{max} is greater than or equal to the y_{max} obtained from the one-dimensional search. The dashed line in the figure illustrates the optimization loop.

Stochastic Simulation Method

The Stochastic-Simulation-Based (SSB) Method is implemented the same way for both linear and nonlinear airplanes. Figure 3 outlines the implementation. There are four major steps in the process:

Step 1. A value of σ_g is selected for the gust filter. Then an approximation to Gaussian white noise is applied to the gust filter producing a time history of stationary Gaussian atmospheric turbulence with a von Karman power spectral density function. The turbulence time history is then applied, by simulation, to the aircraft model, producing a load time history.

Step 2. For each load output, a search of the time history of that load locates "points in time" where peak loads occur. Of these peaks, those which have the largest magnitude within a time span of $\pm\tau_0$ seconds are identified for "extraction." In the extraction procedure, $\pm\tau_0$ second's worth of all of the load time histories and $\pm\tau_0$ second's worth of the corresponding gust time history, centered on

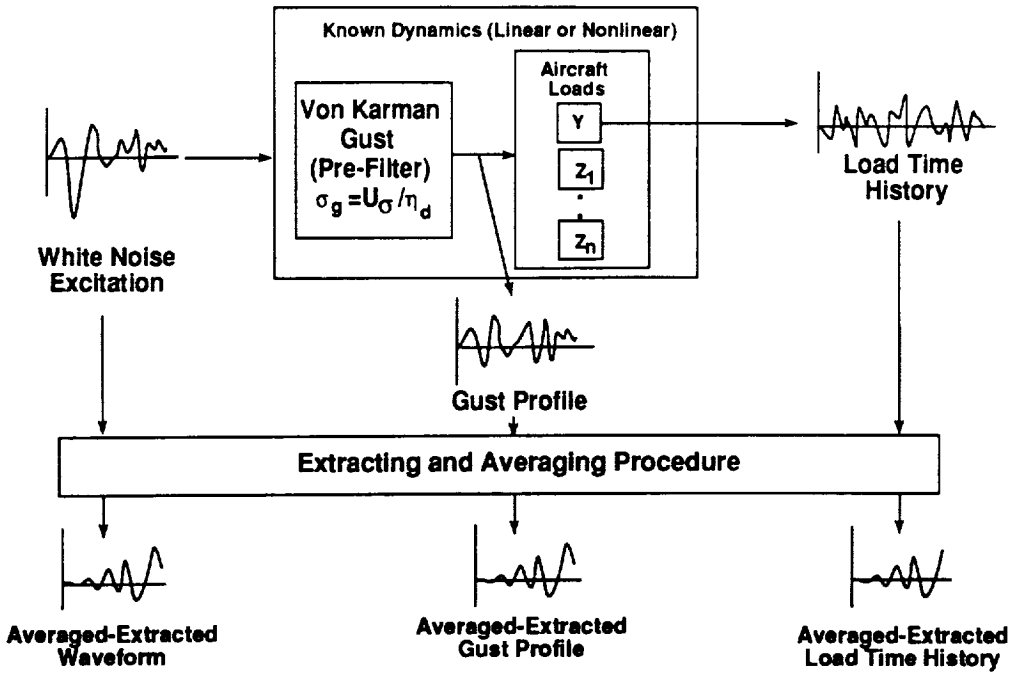

Fig. 3. SSB Method signal flow diagram.

the point in time where the peak occurred, are saved. Figure 4 shows the extraction procedure, where a load time history and the corresponding gust profile time history have been extracted.

Step 3. The extracted load time histories and corresponding gust time histories are "lined up in time" so that each begins at a relative time of zero and each ends $2\tau_0$ seconds later. Figure 5 shows eleven extracted gust and load time histories lined up in time and plotted together. At each point in time the quantities are averaged, producing "averaged-extracted" gust profiles and load time histories.

Step 4. Calculate statistical quantities: level crossings, zero crossings, root-mean-square values.

In reference 5, the extraction performed in step 2 was restricted to loads within ±10% of the MFB answer. Here, that restriction has been removed.

Selection of Gust Intensities

The MFB and SSB Methods both employ the following transfer function approximation of the von Karman power spectral density function (ref. 6)

$$\frac{w_g}{\eta} = \sigma_g \sqrt{\frac{L}{\pi V}} \frac{[1+2.618(L/V)_s][1+0.1298(L/V)_s]}{[1+2.083(L/V)_s][1+0.823(L/V)_s][1+0.0898(L/V)_s]} \quad (1)$$

This expression is referred to in this paper as the gust filter, where the quantity σ_g is the intensity of the gust. In the power spectrum, σ_g is the standard deviation -- which, assuming zero mean, is also equal to the root-mean-square, or RMS, value -- of gust velocity. Both the MFB and the SSB Methods use quantity σ_g as gust intensity. In order to compare the results from the MFB Method with the results from the SSB Method, it is necessary to properly select the gust intensity for each method.

The purpose of this section of the paper is to present the reasoning behind the selection of the values of σ_g for MFB and for SSB Methods so that the results of the two methods may be compared. It will be shown that the gust intensities used for the two analyses differ by a factor of η_d, a design ratio of peak to RMS values.

Design Envelope Criterion. The following equation, from reference 7, expresses the "design value" of quantity y as defined in the design envelope criterion

$$y_{design} = \overline{A}_y U_\sigma \quad (2)$$

where the quantity $\overline{A}y$ is the RMS value of quantity y per unit RMS gust intensity, obtained from a conventional random process analysis of the airplane and U_σ is specified in the criterion. Quantity y_{design} is interpreted as a peak value. From reference 7 the quantity U_σ in equation (2) is shown to be the product of the gust RMS value and the design ratio of peak value of load to RMS value of load, or

$$U_\sigma = \sigma_g \eta_d \quad (3)$$

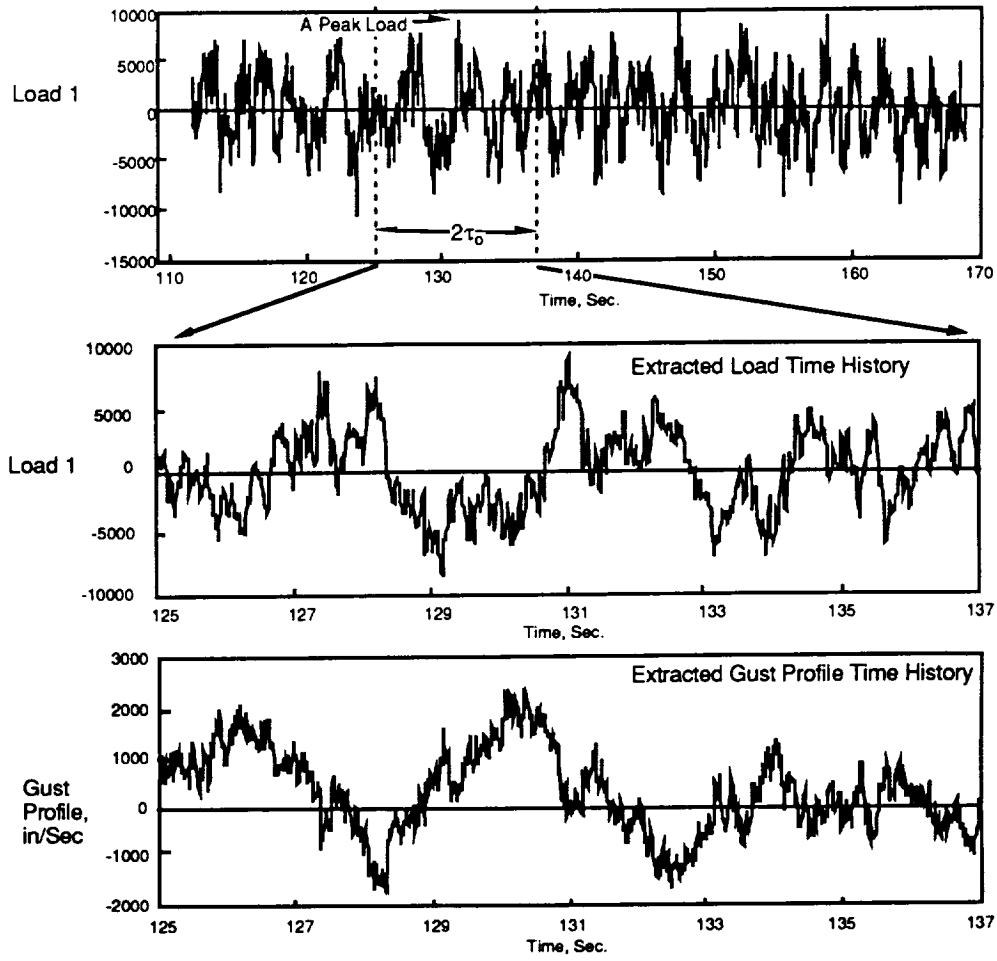

Fig. 4. Extraction procedure for SSB Method.

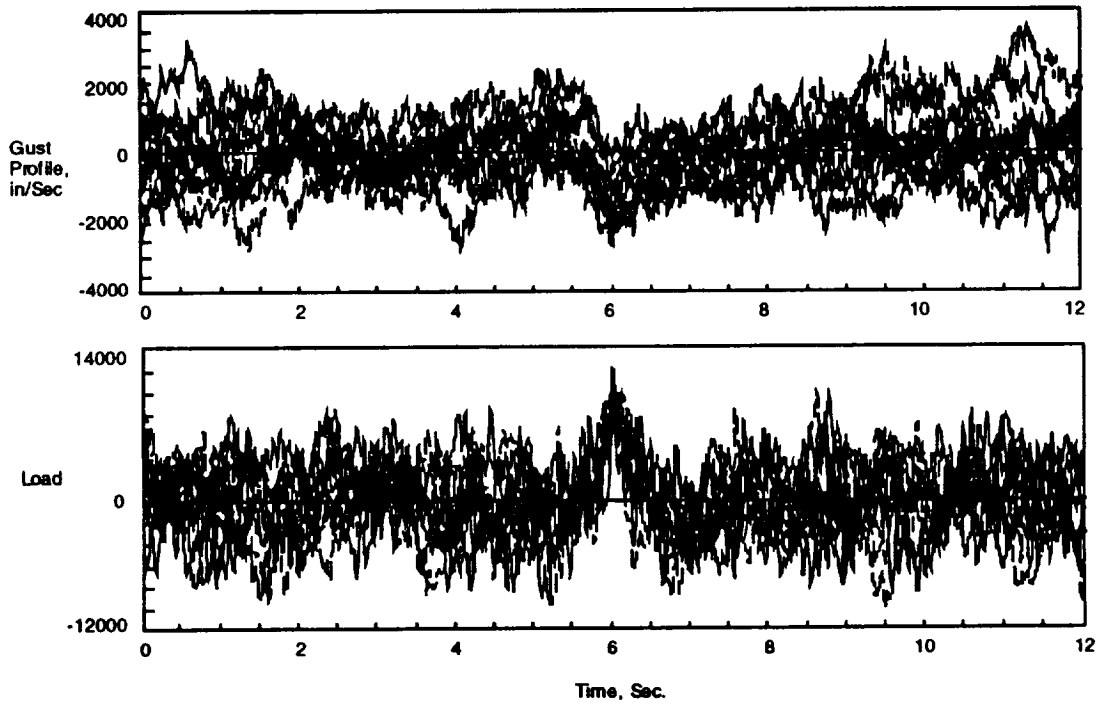

Fig. 5. Extracted gust profile and load time histories.

Although the criterion specifies only the product of, not the breakdown between, σ_g and η_d in equation (3), the breakdown is important in the selection of gust intensities for the SSB Method and, therefore, in comparing MFB and SSB results.

MFB Gust Intensity. Reference 4 shows that, as a consequence of the normalization of the excitation waveform by its own energy and the use of unity gust intensity, the quantity y_{max} from the MFB Linear Method is equal to the quantity $\overline{A}_y$ from a conventional random process analysis, or

$$y_{max}(\sigma_g = 1) = \overline{A}_y \tag{4}$$

In equation (4) y_{max} is interpreted as an RMS value, not a peak value. Substituting equation (4) into equation (2), y_{design} is now

$$y_{design} = y_{max}(\sigma_g = 1)U_\sigma \tag{5}$$

If, in performing the MFB Linear Method, U_σ is used for the gust intensity then the quantity y_{max} is equal to

$$y_{max}(\sigma_g = U_\sigma) = \overline{A}_y U_\sigma \tag{6}$$

The right hand sides of equations (2) and (6) are seen to be equal, therefore

$$y_{design} = y_{max}(\sigma_g = U_\sigma) \tag{7}$$

Two options for the value of σ_g have been offered: $\sigma_g = 1$, for which y_{design} is defined by equation (5); and $\sigma_g = U_\sigma$, for which y_{design} is defined by equation (7). When analyzing a linear system the choice of σ_g is irrelevant because the same value of y_{design} will be obtained in either case. However, when nonlinearities are introduced into aircraft control systems, loads are not simply proportional to gust intensity. Consequently, σ_g should be set to U_σ in the MFB nonlinear calculations, or

$$\sigma_{g\,MFB} = U_\sigma \tag{8}$$

and the resulting "y_{max}" values from the method should be interpreted as y_{design}.

SSB Gust Intensity. In the SSB Method, because random inputs are applied to the simulation, the outputs are already "peaks" in the above sense. Referring again to equation (3) and recalling that the breakdown between σ_g and η_d is not specified (only their product is specified), the following equation can be rewritten for the SSB gust intensity

$$\sigma_{g\,SSB} = \frac{U_\sigma}{\eta_d} \tag{9}$$

To use equation (9) the analyst must select a value for η_d. This approach was applied by Gould in his work with stochastic simulation (ref. 8) in which he used the value of 3 for η_d.

Mathematical Model

A mathematical model of a small two-engine jet transport equipped with a nonlinear yaw damper is used for all the calculations performed in this paper. Figure 6 depicts the nonlinear math model in block diagram form. The portion of the math model that represents the airplane is linear and consists of twelve anti symmetric flexible modes and three rigid-body lateral-directional modes. A doublet lattice code was used to calculate the unsteady aerodynamics for a Mach number of 0.85. These unsteady aerodynamic

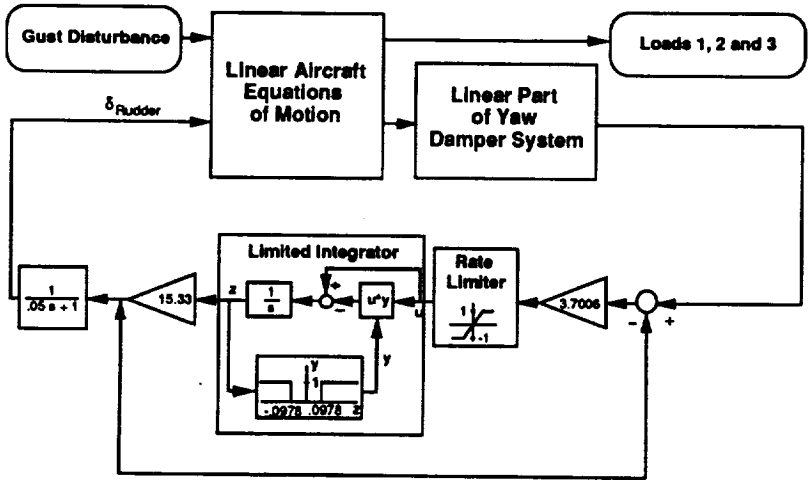

Fig. 6. Block diagram of transport model with nonlinear control system.

forces were converted to the s-plane by evaluating the coefficients of a series proposed by Richardson (ref. 9). An s-plane modeling technique was used to describe the lag states representing the gust penetration and consisted of two states. The basic aeroelastic equations of motion were composed of 75 states for a flight condition at an altitude of 28,000 feet. The yaw damper control system has two nonlinear elements: a rate limiter and a deflection limiter for the rudder. The structure of the yaw damper is shown in the figure. The yaw damper contributed nine additional states to the math model. The final state-space realization had 86 states. The input to the model was lateral gust velocity and the output from the model consists of three loads at the root of the vertical tail. MATRIX$_X$ SYSTEM BUILD[10] was used to construct the nonlinear simulation model.

Results and Discussion

This section of the paper describes numerical results obtained by applying the MFB and SSB Methods to linear and nonlinear models. For the particular nonlinear model chosen for this study unrealistically large values of gust intensity had to be used in order to trigger the nonlinearities present in the system. For purposes of comparing results for linear and nonlinear models, the same large values of gust intensity were used for both.

This section is in four parts. The first describes the calculations performed and presents the nomenclature that will be used throughout this section. The second and third sections discuss the results for the linear and nonlinear models, respectively. The fourth section makes a comparison of the methods.

Summary of Analyses Performed

Table 1 contains a summary of the models used (linear or nonlinear), methods employed (MFB or SSB), and parameter values (σ_g, t_o, τ_o, and T).

For the SSB calculations the same white noise input was used in all the analyses. Also, η_d=3 so that MFB and SSB analyses use gust intensities that differ by a factor of 3 as explained in the Selection of Gust Intensities section of the paper.

Table 1. Calculations performed.

Model Type	Matched-Filter Based			Stochastic-Simulation Based
	Linear	1-dim	Multi-dim	
Linear	**MFB-L** σ_g = 85 ft/s t_o = 10 s	-	-	**SSB$_L$** σ_g= 28.33 ft/s τ_o = 3,6,9,12 s T= 450 s
Nonlinear	-	**MFB-1D** σ_g = 85/170/ 240/255 ft/s t_o = 10 s	**MFB-MD** σ_g = 85 ft/s t_o = 10 s	**SSB$_{NL}$** σ_g= 28.33 ft/s τ_o = 6 s T= 450 s

The bold face titles in the various boxes are to be used when discussing the various results. For example, when MFB-L is cited in the text it refers to the MFB linear analysis of the linear airplane. MFB-1D refers to the one-dimensional search results for the nonlinear model.

Results Using The Linear Model

One of the intents of this paper is to demonstrate, through the numerical results, that the MFB and SSB Methods yield strikingly similar results. Figures 7 and 8 contain the MFB and SSB results for the linear model. In comparing the shapes of the corresponding time-history plots, it is apparent that the results are quite similar. In addition, the load 1 peak values are within 3.8% of each other.

The SSB$_L$ averaged-extracted peaks for load 1 are plotted as functions of τ_o in figure 9. These averaged peaks have been normalized by the load 1 RMS value and are represented by the dots in the figure. Vertical bars and brackets indicating the largest and smallest extracted-normalized peaks have also been provided. The largest-extracted peak is independent of τ_o and is equal to the largest peak in the simulation. The smallest- and the averaged-extracted peaks generally increase with increasing τ_o and approach the largest peak in the simulation record. Theoretically, the largest peak in the simulation increases with increasing simulation length T as the probability of encountering higher and higher peaks increases. For small τ_o values, many peaks near zero will enter the average tending to reduce the averaged-peak value. Thus, by such variations of T and τ_o, there appears to be some latitude in the range of averaged-extracted-peak value that can be obtained.

The data shown in figure 9 for τ_o=6 seconds, corresponds to the data presented in figure 8(b). The value of the normalized-averaged-extracted peak is in the neighborhood of 3. This corresponds to the factor, η_d, that was used in obtaining the SSB gust intensity, and serves to show why the results in figures 7 and 8 are the same. As shown in figure 9, the normalized-averaged-extracted peak for τ_o values other than 6 seconds differ from 3 indicating that the results for those τ_o values would not be the same as the MFB answer.

Results Using Nonlinear Model

The types of nonlinearities of most concern in determining aircraft design loads are control system nonlinearities. For low intensity disturbances, it can be expected that control system nonlinearities will have little effect on the load responses. Thus, the nonlinear response will be much like its linear counterpart. Consequently, any parameter that affects the disturbance level can be expected to have a threshold below which the system behaves linearly.

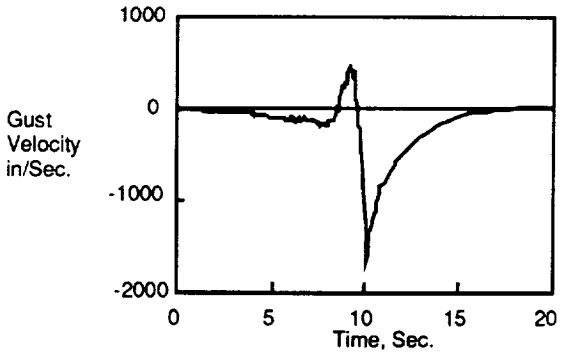

a) Critical gust profile.

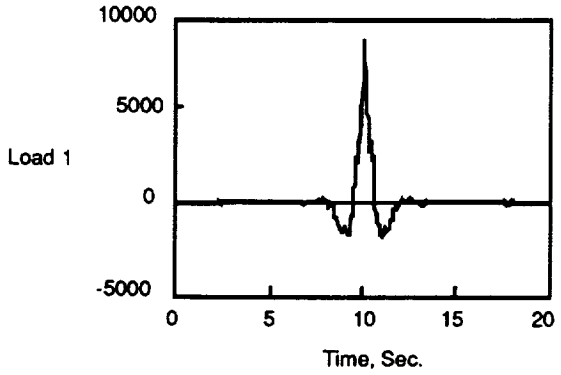

b) Maximized load.

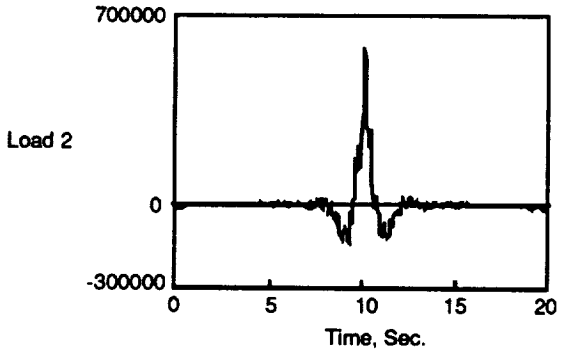

c) Time-correlated load.

Fig. 7. Time histories of key quantities. MFB Linear Method and linear system. t_0=10 sec. σ_g=240 ft./sec.

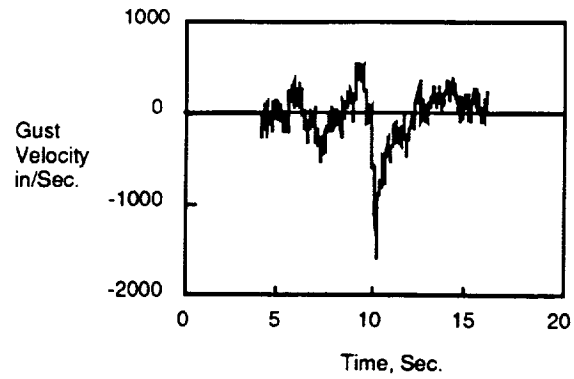

a) Critical gust profile.

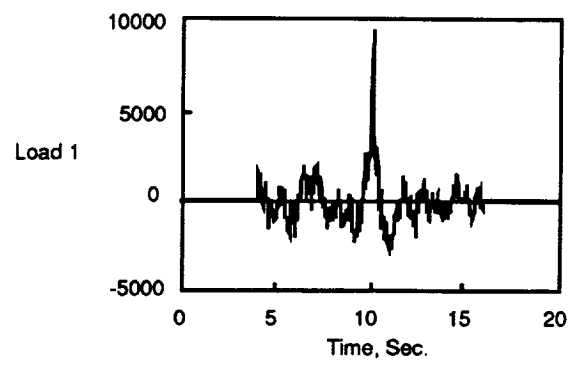

b) Maximized load.

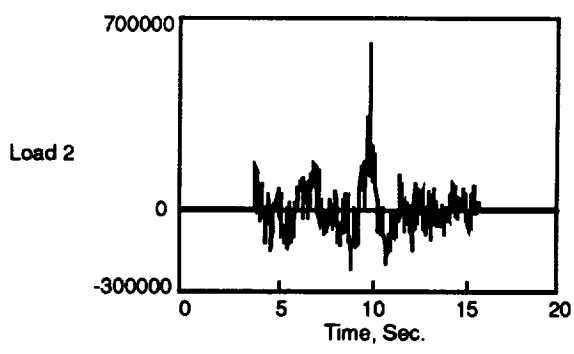

c) Time-correlated load.

Fig. 8. Time histories of key quantities. SSB Method and linear system. τ_0=6 sec. σ_g=80 ft./sec.

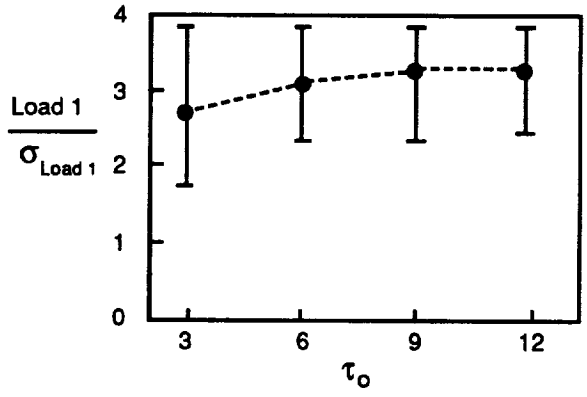

Fig. 9. Effect of τ_0 on load 1 results from SSB Method. Linear system. σ_g=80 ft./sec.

For the methods described in this paper, two parameters affect disturbance intensity. A parameter common to all the analyses was the gust intensity, σ_g. The other parameter was the impulse strength (k) which is only used in the MFB one-dimensional search.

For clarity the parts of this subsection are labeled according to the results discussed.

MFB-1D. Before the MFB-1D results are described and interpreted, a discussion of the general effect of the impulse strength and gust intensity on nonlinear systems is in order.

The variation of the impulse strength (k) affects the MFB-1D analysis by changing the shape of the excitation waveform. For sufficiently low impulse strengths, the shape of the excitation waveform for nonlinear models will be invariant with k. While in this invariant region, the excitation waveform will be the same as that obtained from the linear model. For larger intensities the system nonlinearities will cause the impulse responses and corresponding excitation waveforms to change shape. Consequently, they will no longer be the same as those obtained from the linear system.

The gust intensity affects the one-dimensional search by scaling the excitation waveform prior to being applied to the nonlinear model. Consequently, a low gust intensity should result in the nonlinear model behaving linearly. As gust intensity is increased beyond some threshold the nonlinear model response will begin to deviate from that of its linear counterpart.

One-dimensional search results were obtained at the four gust intensities shown in the box labeled MFB-1D in table 1. Figure 10 shows the results for each of the three loads. Each part of figure 10 contains plots of normalized maximized load as functions of impulse strength: part (a) presents the results for maximizing load 1; part (b) for maximizing load 2; part (c) for maximizing load 3. The normalizing quantity for each load at each value of σ_g is the value of y_{max} obtained from a corresponding MFB linear analysis of the linear model.

With the preceding discussion in mind the results shown in figure 10 will be interpreted, beginning with load 1. The shape of the excitation waveform is invariant for values of k below 1000. As a result, the peak loads are invariant with k for impulse strengths less than this threshold at all the gust intensities.

At the lowest gust intensity (85 ft/sec) the largest load obtained from the analysis is obtained at the low values of k. In addition, the ratio of ymax nonlinear to y_{max} linear is unity for these low k values. This indicates that the nonlinear model behaves linearly for load 1 at this gust intensity.

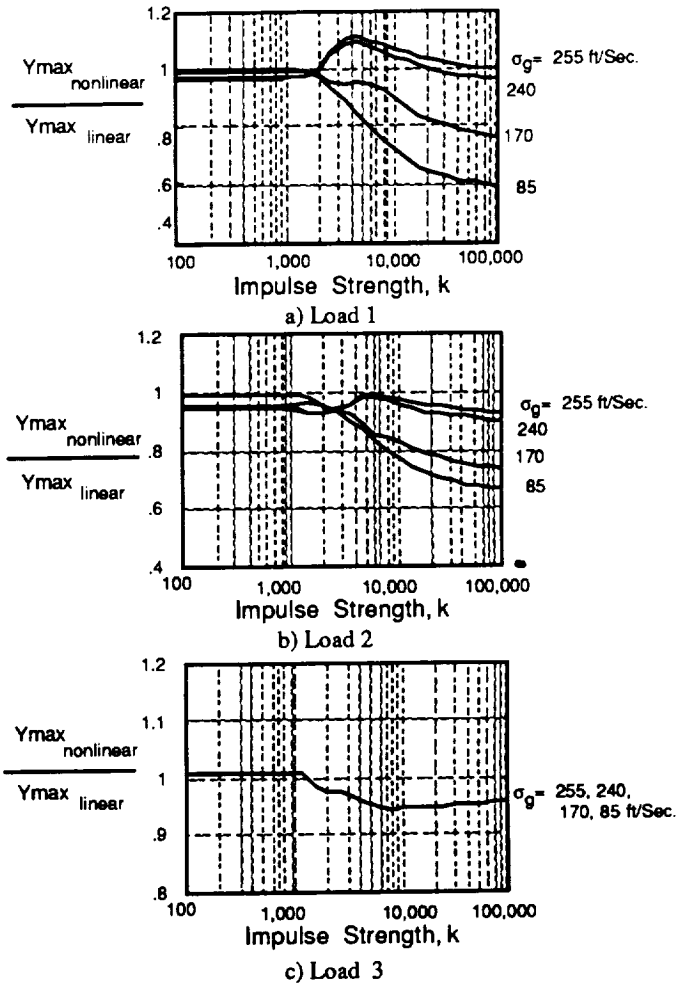

Fig. 10. Normalized maximum loads as functions of impulse strength. MFB One-Dimensional Method. t_0=10 sec.

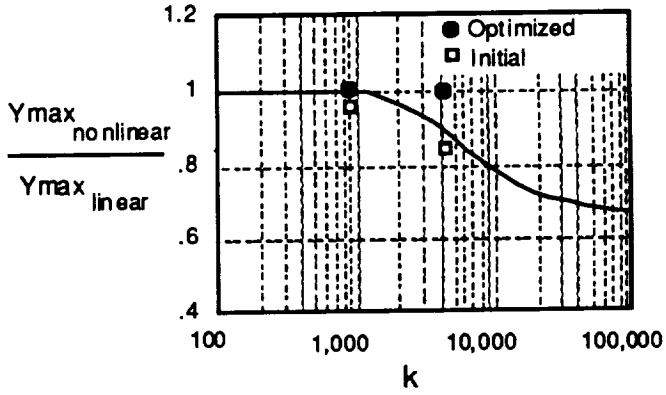

Fig. 11 Normalized maximum loads for load 2. MFB Multi-Dimensional Method. t_0=10 sec. σ_g=240 ft./sec.

At sufficiently large gust intensities the peak value of load 1 occurs at an impulse strength greater than 1000, with a ratio of ymax nonlinear to ymax linear being larger than in the invariant region. This indicates that the nonlinearity has a significant effect on the load, and is of great importance at this gust intensity.

Similar trends are noted for load 2 in figure 10. Load 3, on the other hand, is invariant with gust intensity, and the largest load is obtained for low values of k. This indicates that the nonlinear control system has very little effect on load 3 at all the gust intensities investigated.

MFB-MD. Two separate multi-dimensional searches were performed on the nonlinear transport model to maximize load 2 at a gust intensity of 85 ft./sec. The number of design variables used in the optimization procedure was 160. Reference 4 gives a detailed description of what the design variables represent and how to select the proper number to use.

These MFB-MD results are shown plotted with the corresponding MFB-1D curve from figure 10(b). While the value of k has no bearing on the multi-dimensional result, the location of each of the two sets of starting and ending points with respect to the k-axis indicates the value that was used to generate the starting excitation waveform for the search. The first search used, as the initial condition, the critical gust profile corresponding to an impulse strength of 900; the other, the critical gust profile corresponding to an impulse strength of 4300. The initial conditions are depicted in the figure by open symbols; the optimized results, by closed symbols.

The MFB-MD results indicate that, for this particular load and gust intensity, the multi-dimensional search increased the maximum value of load 2 no more than the highest value achieved by the one-dimensional search. In this instance, then, the one-dimensional search was sufficient to provide the maximized load.

Comparison of MFB-1D and SSB_N. Again keeping in mind that one of the intents of this paper is to demonstrate that the MFB and SSB Methods yield similar results, a comparison can be made of the nonlinear time histories. Figures 12 and 13 contain the MFB-1D and SSB_N results, respectively. These analyses were performed with U_σ= 240 ft./sec. As with the analogous linear results, the time-history plots obtained using in the MFB-1D and SSB_N calculations for the nonlinear model are quite similar in shape and peak load value. Thus, the one-dimensional search obtained the worst case gust profile for the nonlinear model without the need for MFB multi-dimensional search.

By comparing the linear results in figures 7 and 8 with the nonlinear results in figure 12 and 13, a significant difference is noted between the linear results and the nonlinear results. This observation indicates that there is a substantial difference between the linear and nonlinear response at this U_σ value. This indicates the need for using methods capable of handling the nonlinearities. This result is also consistent with the one-dimensional search prediction that the nonlinearities would significantly affect aircraft response at this U_σ value. These observations suggest that the MFB one-dimensional search is capable of efficiently locating the worst case gust profile and corresponding maximized load.

Comparison of SSB_N and SSB_L. To further explore the effect of gust intensity on the response of the nonlinear aircraft the normalized load level exceedences were extracted from the SSB linear and nonlinear analyses time histories. Figure 14 shows the level crossing results of both the SSB_N and SSB_L analyses for each of the three loads. For each load, the solid line represents the theoretical level-crossing curve predicted by Rice's equation. The symbols represent the number of crossings of various load levels. The load levels have been normalized by corresponding σ_g values.

Figure 14 shows the linear results and the nonlinear results at the lower gust intensity (28.33 ft./sec.) to be essentially the same. This is consistent with the one-dimensional search prediction where the largest load was obtained in the invariant region, indicating linear behavior of the nonlinear model.

The load 1 and load 2 linear results and the nonlinear results at the larger gust intensity (80 ft./sec.) differ significantly at large load values. Again, these results are consistent with the one-dimensional search prediction where the largest loads obtained for loads 1 and 2 did not occur in the invariant region, thus indicating the importance of the nonlinearity.

Figure 14 shows the load 3 linear results and the nonlinear results at all the gust intensities to be quite similar. This is consistent with the one-dimensional search prediction where the largest load was obtained in the invariant region and the nonlinearity had little effect on this load.

Comparison of Efficiencies of the MFB and SSB Methods

Two measures may be used to compare the efficiency of the MFB and SSB Methods. One is the amount of computer storage required, and the other is the amount of CPU time required to perform the calculations. The SSB Method required approximately 25 times more storage than the MFB Methods, and table 2 shows a comparison of the approximate total seconds of simulation required to perform a complete analysis for this model at one gust intensity.

Table 2. Comparison of simulation time required.

Model Type	Matched-Filter Based			Stochastic-Simulation Based
	Linear	1-dim	Multi-dim	
Linear	60 Sec	-	-	450 Sec
Nonlinear	-	300 Sec	10,800 Sec	450 Sec

For the linear model, the MFB Method is more efficient than the SSB Method. For nonlinear systems the MFB multi-dimensional search is much more expensive that the SSB Method, while the MFB one-dimensional search requires less time that the SSB Method. The SSB Method requires the same amount of simulation time for both linear and nonlinear models.

Since the multi-dimensional search is prohibitively expensive, the practical options for methods applicable to nonlinear systems are the MFB one-dimensional search and the SSB Method. Based on the preceding discussion, the one-dimensional search is able to predict the maximized loads for nonlinear systems. In addition, it requires less computer resources than the SSB Method. These factors point to the MFB one-dimensional search as a means of replacing or at least complementing stochastic approaches.

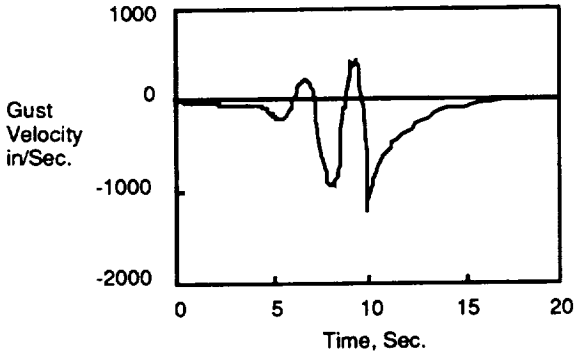

a) Critical gust profile.

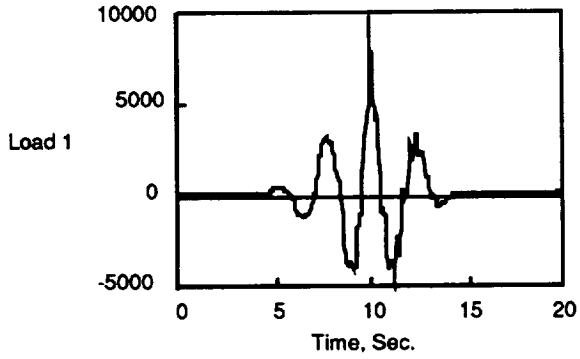

b) Maximized load.

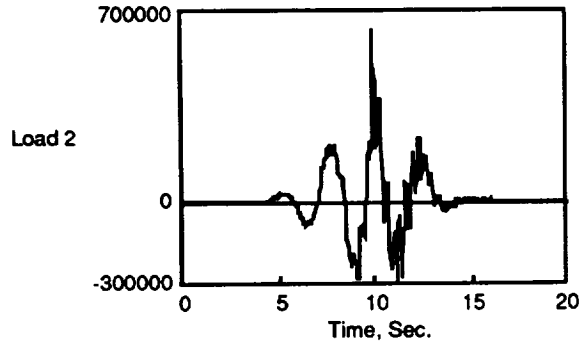

c) Time-correlated load.

Fig. 12. Time histories of key quantities. MFB One-Dimensional Method and nonlinear system. t_0=10 sec. σ_g=240 ft./sec.

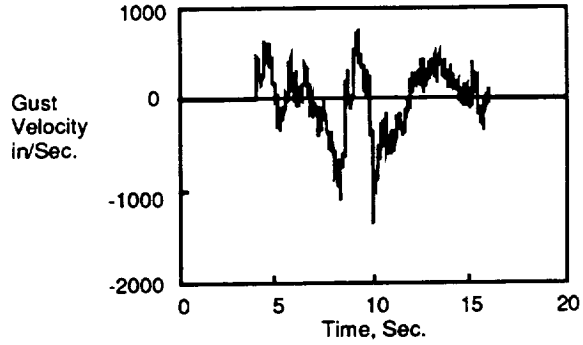

a) Critical gust profile.

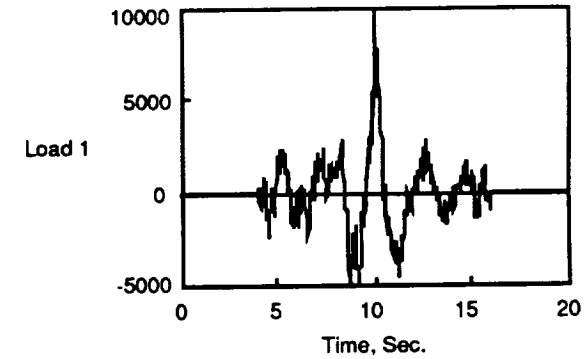

b) Maximized load.

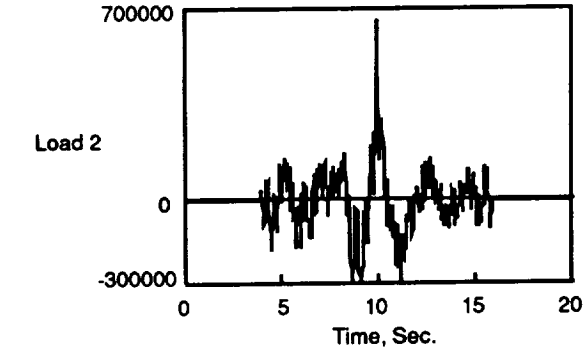

c) Time-correlated load.

Fig. 13. Time histories of key quantities. SSB Method and nonlinear system. τ_0=6 sec. σ_g=80 ft./sec.

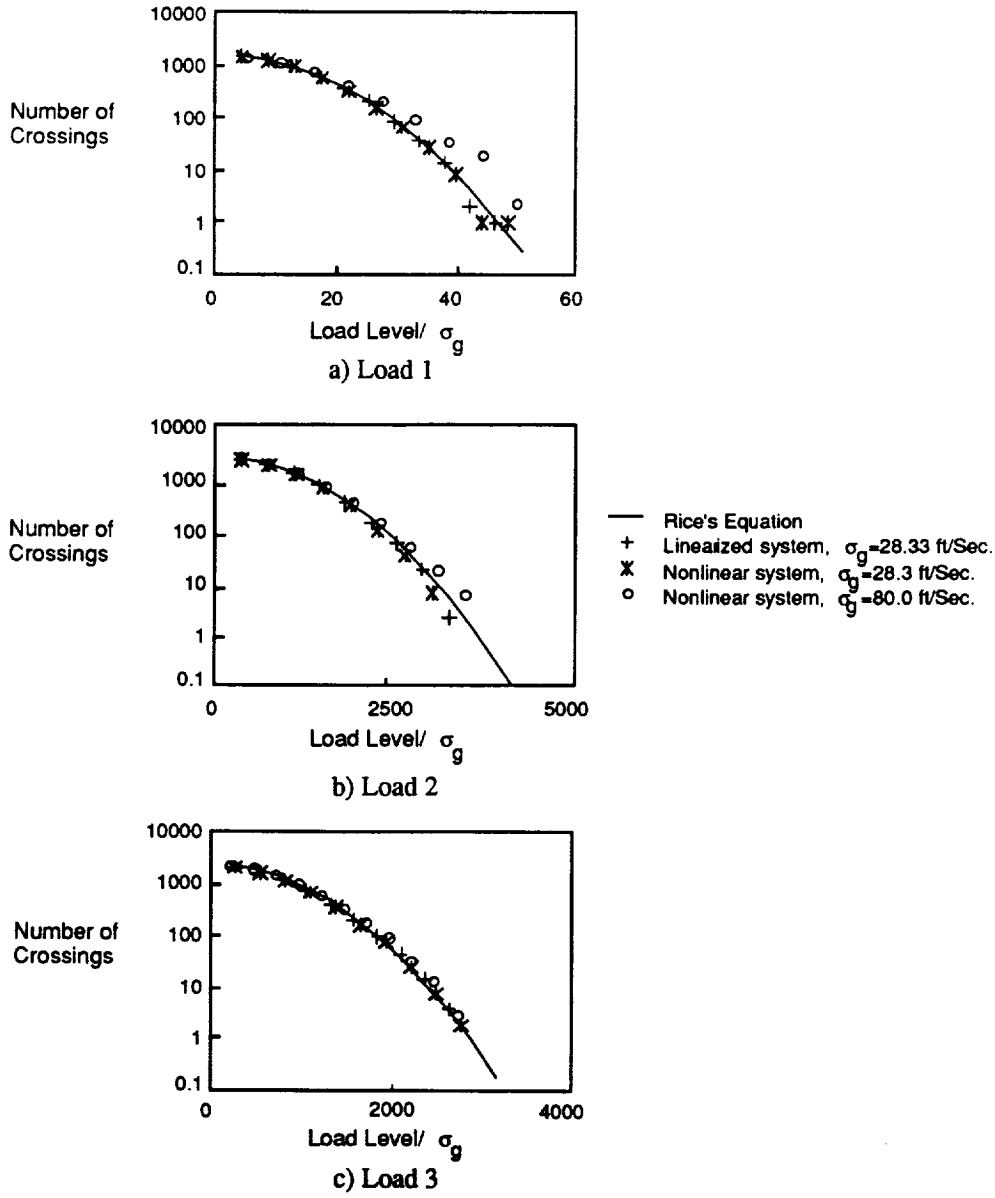

Fig. 14. Number of level crossings from SSB Method.

Concluding Remarks

This paper has described two analysis methods -- one deterministic, the other stochastic -- for computing maximized and time-correlated gust loads for aircraft with nonlinear control systems. The methods, the Matched-Filter-Based (MFB) Method and the Stochastic-Simulation-Based (SSB) Method, were applied to a mathematical model of a current transport aircraft equipped with a nonlinear yaw damper.

The results predicted by the two methods are strikingly similar and demonstrate that the key quantities from the MFB Method (viz. critical gust profile, maximized load, and time correlated load) are realizable in the SSB Method. Another significant finding is the relative computational costs of performing analyses using the MFB and SSB Methods. Based on the total amount of simulation time required to obtain maximized and time correlated loads, the SSB Method costs about one and a half times as much as the MFB one-dimensional search. The cost for the MFB multi-dimensional search is about one and a half orders of magnitude more than cost of the MFB one-dimensional search.

References

1. Perry, Boyd III; Pototzky, Anthony S.; and Woods, Jessica A.: NASA Investigation of a Claimed "Overlap" Between Two Gust Response Analysis Methods. Journal of Aircraft, Vol. 27, No. 7, July 1990, pp. 605-611.

2. Pototzky, Anthony S.; Zeiler, Thomas A.; Perry, Boyd III: Calculating Time-Correlated Gust Loads Using Matched Filter and Random Process Theories. Journal of Aircraft, Vol. 28, No. 5, May 1991, pp. 346-352.

3. Zeiler, Thomas A.; Pototzky, Anthony S.: On the Relationship Between Matched Filter Theory as Applied to Gust Loads and Phased Design Loads Analysis. NASA CR- 181802, April 1989.

4. Scott, Robert C., Pototzky, Anthony S., and Perry, Boyd III: Maximized Gust Loads For a Nonlinear Airplane Using Matched Filter Theory and Constrained Optimization. NASA TM-104138, June 1991.

5. Scott, Robert C., Pototzky, Anthony S., and Perry, Boyd III: Determining Design Gust Loads For Nonlinear Aircraft - Similarity Between Methods Based on Matched Filter Theory and on Stochastic Simulation. NASA TM-107614, April 1992.

6. Barr, N. M.; Gangsaas, D.; and Schaeffer, D. R.: Wind Tunnel Models for Flight Simulator Certification of Landing and Approach Guidance and Control Systems. Boeing Commercial Airplane Co., Seattle, WA. Final Report FAA-RD-74-206, 1974.

7. Hoblit, Frederic M.: Gust Loads on Aircraft: Concepts and Applications. American Institute of Aeronautics and Astronautics, Washington, 1988.

8. Gould, J. D.: Effects of Active Control System Nonlinearities on the L-1011-3(ACS) Design Gust Loads. AIAA Paper No. 85-0755, 1985.

9. Richardson; J. R.: A More Realistic Method For Routine Flutter Calculations. AIAA Symposium on Structural Dynamics, August 1965.

10. SYSTEM_BUILD 7.0 User's Guide: Integrated Systems Inc. October 1988.

REPORT DOCUMENTATION PAGE

Form Approved
OMB No. 0704-0188

1. AGENCY USE ONLY (Leave blank)	2. REPORT DATE	3. REPORT TYPE AND DATES COVERED
	July 1993	Technical Memorandum

4. TITLE AND SUBTITLE
Further Studies Using Matched Filter Theory and Stochastic Simulation for Gust Loads Prediction

5. FUNDING NUMBERS
WU 505-63-50-15

6. AUTHOR(S)
Robert C. Scott, Anthony S. Pototzky, and Boyd Perry III

7. PERFORMING ORGANIZATION NAME(S) AND ADDRESS(ES)
NASA Langley Research Center
Hampton, VA 23681-0001

8. PERFORMING ORGANIZATION REPORT NUMBER

9. SPONSORING / MONITORING AGENCY NAME(S) AND ADDRESS(ES)
National Aeronautics and Space Administration
Washington, DC 20546-0001

10. SPONSORING / MONITORING AGENCY REPORT NUMBER
NASA TM-109010

11. SUPPLEMENTARY NOTES
Presented at the AIAA 34th Structures, Structural Dynamics, and Materials Conference, 4/19-21/93, LaJolla, CA. Scott and Perry: NASA Langley Research Center, Hampton, VA.; Pototzky: Lockheed Engineering and Sciences Co., Hampton, VA.

12a. DISTRIBUTION / AVAILABILITY STATEMENT
Unclassified - Unlimited

Subject Category 05

12b. DISTRIBUTION CODE

13. ABSTRACT *(Maximum 200 words)*

This paper describes two analysis methods -- one deterministic, the other stochastic -- for computing maximized and time-correlated gust loads for aircraft with nonlinear control systems. The first method is based on matched filter theory; the second is based on stochastic simulation. The paper summarizes the methods, discusses the selection of gust intensity for each method and presents numerical results. A strong similarity between the results from the two methods is seen to exist for both linear and nonlinear configurations.

14. SUBJECT TERMS
matched filter theory; gust loads; dynamic loads; nonlinear model; time-correlated loads; stochastic simulation

15. NUMBER OF PAGES
14

16. PRICE CODE
A03

17. SECURITY CLASSIFICATION OF REPORT	18. SECURITY CLASSIFICATION OF THIS PAGE	19. SECURITY CLASSIFICATION OF ABSTRACT	20. LIMITATION OF ABSTRACT
Unclassified	Unclassified		